Analyzing the potential of ASCAT Surface Soil Moisture 6.25 km over Mexico for agricultural drought monitoring.

Dariela Amaranta Vazquez Rodriguez, Pavan Muguda Sanjeevamurthy, Wolfgang Wagner, Sebastian Hahn

September 4, 2024

Report on ASCAT SSM for Agricultural Drought Monitoring in Mexico

Table of Contents

List of Figures

List of Acronyms

ASCAT	Advanced SCATterometer on-board Metop
CGLS	Copernicus Global Land Service
CONAGUA	National Comision of Water in Mexico *
HSAF	EUMETSAT Satellite Application Facility on Support to Operational Hydrology and Water Management
IMTA	Mexican Institute of Water Technology *
INEGI	National Institute of Statistics and Geography of Mexico *
LPRM	Land Parameter Retrieval Model
LST	Land Surface Temperature
MSG	Metosat Second Generation
MSM	Mexico drought monitor *
SMA	Soil Moisture Anomaly
SMAPI	Soil Moisture Anomaly Percentage Index
SMN	National Service of Meteorology of Mexico *
SSM	Surface Soil Moisture
SPEI	Standardized Precipitation and Evapotranspiration Index
SPI	Standardized Precipitation Index

***** By its initials in Spanish

1 Introduction

Mexico has been experiencing intense and frequent drought in recent times due to intensifying climate change. In 2002 the National Commission of Water (CONAGUA) and the National Meteorological Service (SMN) created the “Mexico Drought Monitor” (MSM for its initials in Spanish) to identify, quantify, and map the areas under drought conditions by the implementation of the Standardized Precipitation Index (SPI) using radar and rain gauges data. However, it was not until 2014 that fortnightly and monthly reports on drought conditions began for the country [CONAGUA & SMN, 2024].

The Mexico Drought Monitor (MSM) and the Annual Climate Report identified the years 2011, 2012, 2020, 2021, and 2023 as among the driest, marked by extensive drought conditions. The drought event spanning 2011-2012 is noted as the most severe in recent Mexico’s history, affecting 85% of the country's territory, with 47% of the area experiencing exceptionally severe conditions. The second most severe drought occurred in 2020 – 2021 and lasted eleven consecutive months, affecting 65% of the national territory and with a 2.7% deficit in annual cumulative precipitation. The most recent event is the one that started in June 2023, and that apparently persisted till May 2024. 2023 was the driest year in the last 80 years in which 30% of the national territory present extreme and exceptional extreme drought conditions during September.

In Mexico, the monitoring and analysis of drought are predominantly focused on precipitation deficits, often overlooking other critical factors such as soil moisture, streamflow in both surface and groundwater, and reservoir water levels. This narrow focus has lead to an incomplete understanding of the drought phenomenon and its short- and long-term impacts. Reports typically conclude that drought is over when a significant portion of the territory experiences its first rainfall event, without accounting for the low soil moisture levels and their implications for agriculture.

Additionally, Mexico lacks a comprehensive network of in-situ soil moisture stations, relying primarily on limited streamflow and meteorological stations for drought monitoring. To address this gap, recent research projects have focused on evaluating satellite-derived soil moisture products such the NASA Soil Moisture Active Passive (SMAP) in specific regions. Given the limitations of official in-situ observations, these projects often conduct their own measurements over short periods to assess the accuracy of soil moisture estimates provided by satellite soil moisture products [A. Monsiváis-Huertero *et al*., 2022].

In 2015, the Mexican Institute of Water Technology (IMTA, by its initials in Spanish) conducted an analysis of SMOS (Soil Moisture and Ocean Salinity) for potential national coverage applications. However, the study concluded that the satellite data required further calibration and post-processing to align with in-situ observations. Despite the promising potential, IMTA lacks the necessary resources and support to implement this calibration effectively. This limitation constrains the evaluation and calibration of soil moisture satellite products across Mexico, particularly in relation to precipitation data and cross-validation with other soil moisture products [Lobato-Sanchez, R., 2015].

Building on this premise, the current study presents an analysis of the Advanced Scatterometer (ASCAT) Surface Soil Moisture (SSM) at 6.25 km sampling product across various climate and agricultural zones in Mexico. The objective is to evaluate the performance of ASCAT SSM in assessing soil moisture conditions by cross-validating its results with ERA5-Land and ESA CCI datasets. Additionally, this study examines the potential of ASCAT SSM derived drought indicators such has soil moisture anomaly percentage index (SMAPI) and soil moisture anomaly z-scores to detect drought conditions by comparing against conventional precopotaton based drought indices such as the Standardized Precipitation Index (SPI) by [CONAGUA & SMN, 2024] and the Standardized Precipitation Evapotranspiration Index (SPEI) by [Peng et al., 2023].

Following is the brief outline of this report:

Section 2: provides an overview of Mexico's physiographic characteristics and geographic location, with a particular emphasis on its climatic zones, land cover classes and rainfall patterns during the wet season

Section 3: highlights the challenges associated with subsurface scattering effects on soil moisture measurements. Additionally, it evaluates the temporal quality of ASCAT soil moisture dataset by comparing it with other established soil moisture products, to evaluate its consistency and reliability over time.

Section 4: details the similarities between the anomalies delivered by ASCAT dataset and precipitation anomalies from the MDM. Also evaluate the spatial similarity in drought severity classification by the comparison from SMAPI and ZScore from ASCAT, SPEI from CEDA, and SPI by the Mexico Drought Monitor.

Section 5: summarizes the findings of the report.

2 Study Area: Mexico

Mexico is located in North America between the latitudes 14º N to 32º N, and longitudes 86º W to 117º W. The country is primarily composed of mountain ranges, valleys, and plateaus, which cover 85% of the territory. The remaining 15% consists of coastal plains and the Yucatan Peninsula.

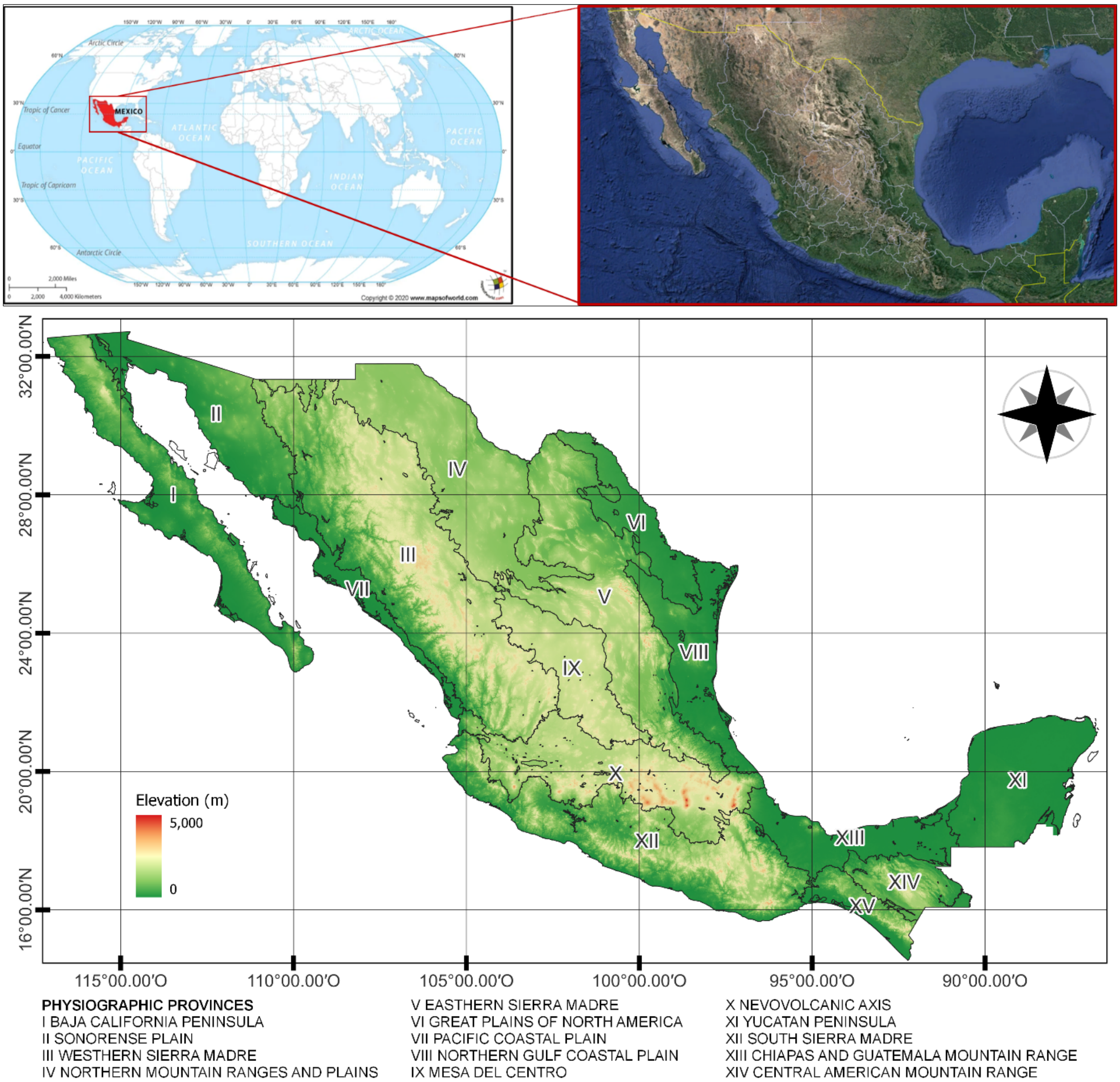

Figure 1. Physiographic Regions and Elevations of Mexico

The territory is formed by 14 physiographic provinces, the principal composed by the largest mountain ranges known as "Sierra Madre" (Mother Mountain Range). Mexico has five major mountain ranges that cross the country predominantly from north to south, these are the Eastern Sierra Madre, Western Sierra Madre, South Sierra Madre, and Chiapas and Guatemala Mountain Range. Additionally, the Trans-Mexican Volcanic Belt or the Neovolcanic Axis encircles Central Mexico.

2.1 Climate

According to Koppen Climates, Mexico has 16 types of climates across the country as shown in Figure 2. The Tropic of Cancer divides the country into temperate arid zones and tropical zones, in which climate varies in function of the elevation. The arid region of Mexico is situated between the Western Sierra Madre and Eastern Sierra Madre in northern Mexico, with mostly temperate climates over mountains. Central and South Mexico have more temperate climate mostly in high elevations and tropical climates over coastal areas and over the Chiapas and Guatemala Mountain Range.

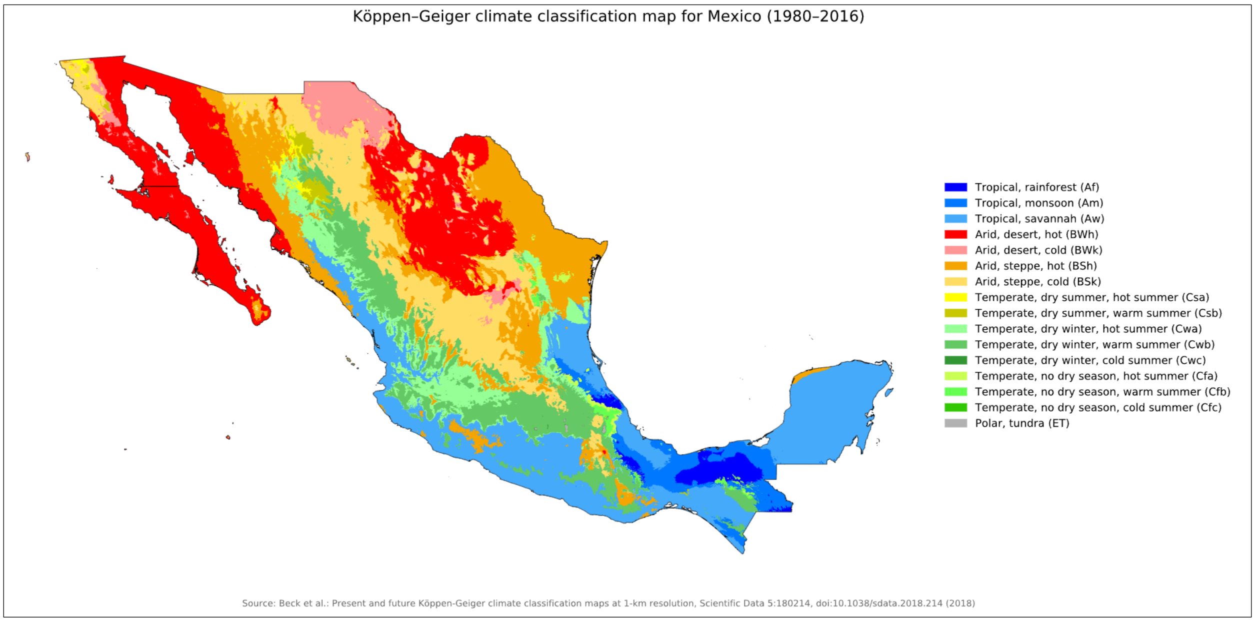

Figure 2 Koppen Climate classification of Mexico (1980 - 2016)

Mexico has pronounced wet and dry seasons. Figure 3 shows that the country experiences a rainy season from June to October and significantly less rain during the remainder of the year. February and July generally are the driest and wettest months, respectively. According to the climatology of the last 30 years, July, August and September presents the higher presences of precipitation, while February, March and April are the driest months of the year (with less than 20 mm of accumulative precipitation).

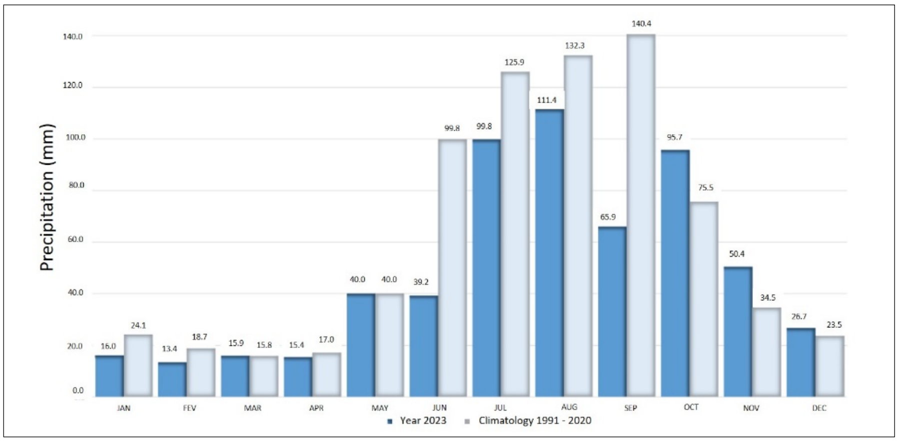

Figure 3 2023 Monthly Precipitation vs Climatology from 1991 -2020

In addition, Figure 4 shows the annual precipitation percentages since 1940. The figure shows that the wettest years are 2008, 2010, 2013, and 2015. On the other hand, years with deficit of precipitation or driest years are 2011, 2019, 2020, 2021, and 2023.

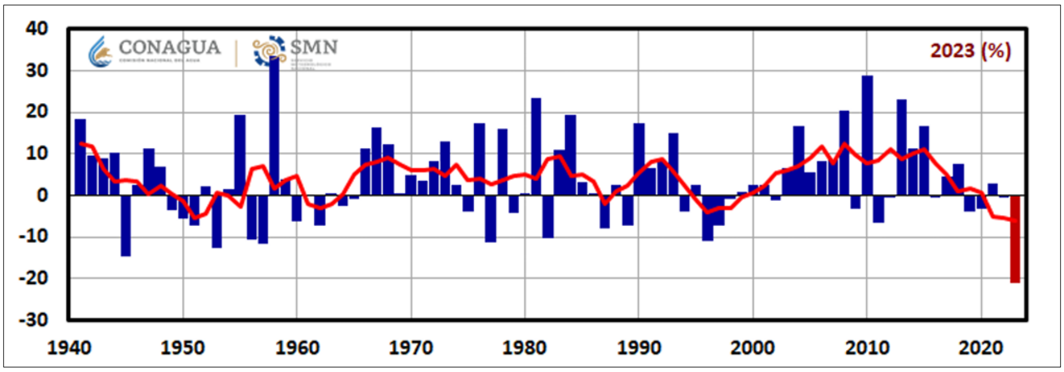

Figure 4 National Annual Precipitation Percentages (blue bars) and Five-Year Moving Average (red line) from 1940 to 2023. (Data from CONAGUA and SMN)

2.2 Land Cover and Vegetation

The physiographic and climatic conditions of Mexico play a crucial role in shaping the distribution and development of vegetation and land cover across the country. The National Institute of Statistics and Geography (INEGI) has produced a national map of land cover and vegetation (Figure 5). This map highlights that central Mexico's land cover is primarily a mix of rainforest and rainfed agriculture, while irrigated agriculture is predominant in the northern regions of the country.

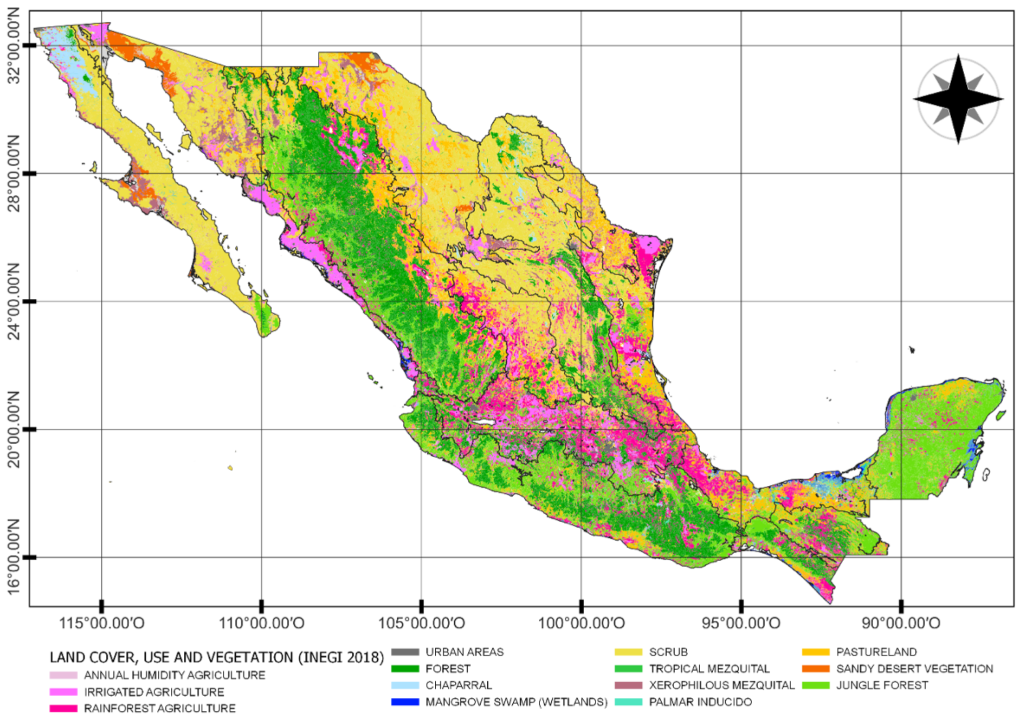

Figure 5. Land cover, use and vegetation in Mexico by INEGI 2018

Figure 5 illustrates that forested areas dominate the mountainous regions in northern Mexico, while the southern mountain ranges are characterized by a combination of forest and tropical rainforest. In contrast, the arid and semi-arid regions are predominantly covered by shrubland, pastureland, and desert vegetation, including sand dunes.

3 HSAF Surface Soil Moisture 6.25 km Analysis

The analysis aims to evaluate the quality of HSAF surface soil moisture by comparing it with other soil moisture datasets like ERA5 and ESA CCI SM (passive). To achieve this, time series data from 2007 to 2022 are examined for correlations to understand the temporal quality and underlying effects of subsurface scattering in arid and semi-arid climatic zones. Furthermore, to ensure consistency for the analysis, the SM datasets of ERA5 and ESA CCI passive are harmonized with the HSAF SSM data (both spatially and temporally).

3.1 Overview of products

Following is the overview on the data products used for HSAF soil moisture analysis:

3.1.1 HSAF Surface Soil Moisture 6.25km [Wagner et al, 2013]

HSAF Surface Soil Moisture (SSM) 6.25km data is derived from the backscatter observations of the Advanced SCATterometer (ASCAT) onboard Metop A, B, and C satellites. The generation of ASCAT SSM data relies on the TU Wien change detection algorithm, which assumes a linear relationship between scatterometer backscatter and soil moisture. Even though the algorithm accounts for factors such as surface roughness, topography, and vegetation as invariant over the years, seasonal variations in vegetation are corrected through the multi-angle viewing capabilities of ASCAT. The soil moisture data is organized on a fixed Earth Fibonacci grid, consisting of 5° x 5° cells with grid points evenly distributed at a sampling interval of 6.25 km. Each grid point corresponds to a spatial resolution of approximately 10-15 km x 10-15 km.

3.1.2 ERA5-Land [Hersbach et al., 2020]

ERA5-Land is a global climate and weather reanalysis dataset released by the European Centre for Medium-Range Weather Forecasts (ECMWF) as part of the Copernicus Climate Change Service (C3S). The dataset contains over 50 surface parameters at a 9 km Gaussian grid scale, with hourly temporal frequency, available from 1950 and up to 5 days behind real-time. The data is derived from various satellite measurements and meteorological observations, using advanced data assimilation techniques to produce accurate and reliable estimates.

3.1.3 ESA CCI SM (passive) [Dorigo et al. 2017]

The data has been developed as part of the ESA's program to monitor essential climate variables worldwide, known as the Climate Change Initiative (CCI). The ESA CCI SM data is obtained from brightness temperature observations collected by various passive microwave sensors using the microwave radiative transfer model called the Land Parameter Retrieval Model (LPRM). The soil moisture data has a spatial resolution of 0.25 degrees and is provided with daily temporal resolution in NetCDF global images. The available data spans 40 years, from 1978 to 2022.

3.2 Correlation Analysis

The Pearson Correlation test results, as shown in Figure 6, reveal the correlation values for the entire time series. It is evident that a significant portion of the Mexican territory exhibited Pearson correlation coefficients above 0.6 with ERA5, while correlations with ESA CCI were generally above 0.4. These lower correlations are due to data gaps in the ESA CCI passive product which leads to a lesser number of valid observations for computing Pearson correlation coefficient with ASCAT data.

Additionally, negative correlations are particularly evident in the arid and semiarid regions in north Mexico, as well as in the southeastern wetlands of the Yucatan Peninsula. It is well-established that these climatic zones are susceptible to backscattering issues, as documented in [Wagner et al., 2022] and [Wagner et al. 2024].

In contrast, the western part of the country demonstrated the highest correlation values with ERA5, otherwise ESA CCI exhibited the lowest correlation values in the region, likely due to data gaps.

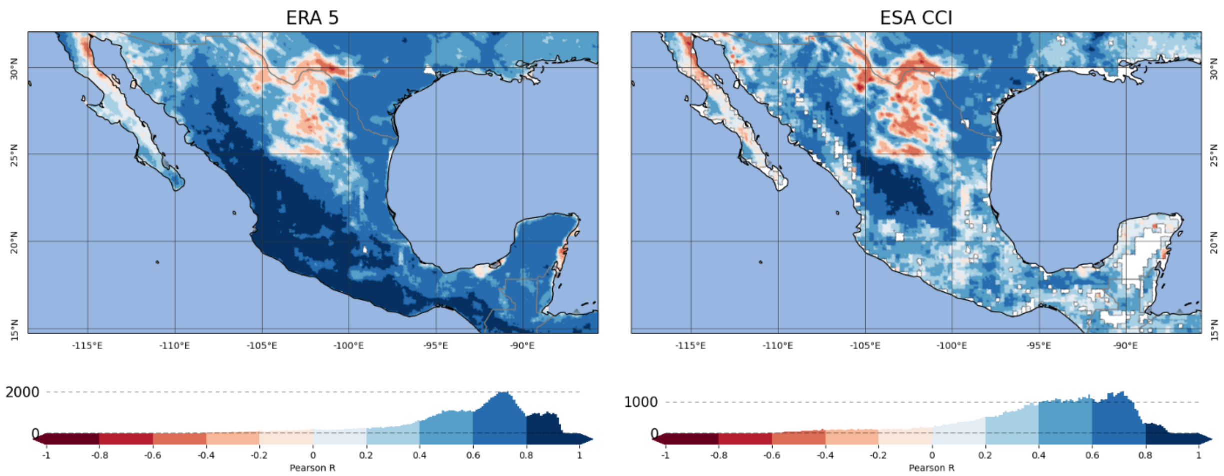

Figure 6. Pearson Correlations for entire time series

Arid and semiarid regions examples can be appreciated in Figure 7 to Figure 10. Figures 7 and 8 present bare land areas, while figures 9 and 10 show irrigated agricultural zones. The performance in arid and semiarid bare land zones illustrated in Figure 7, shows an arid desert zone situated between mountainous regions. On the other hand, Figure 8 depicts an arid desert along the coast of the Baja California Gulf. Both regions are primarily composed of leptosols and regosols.

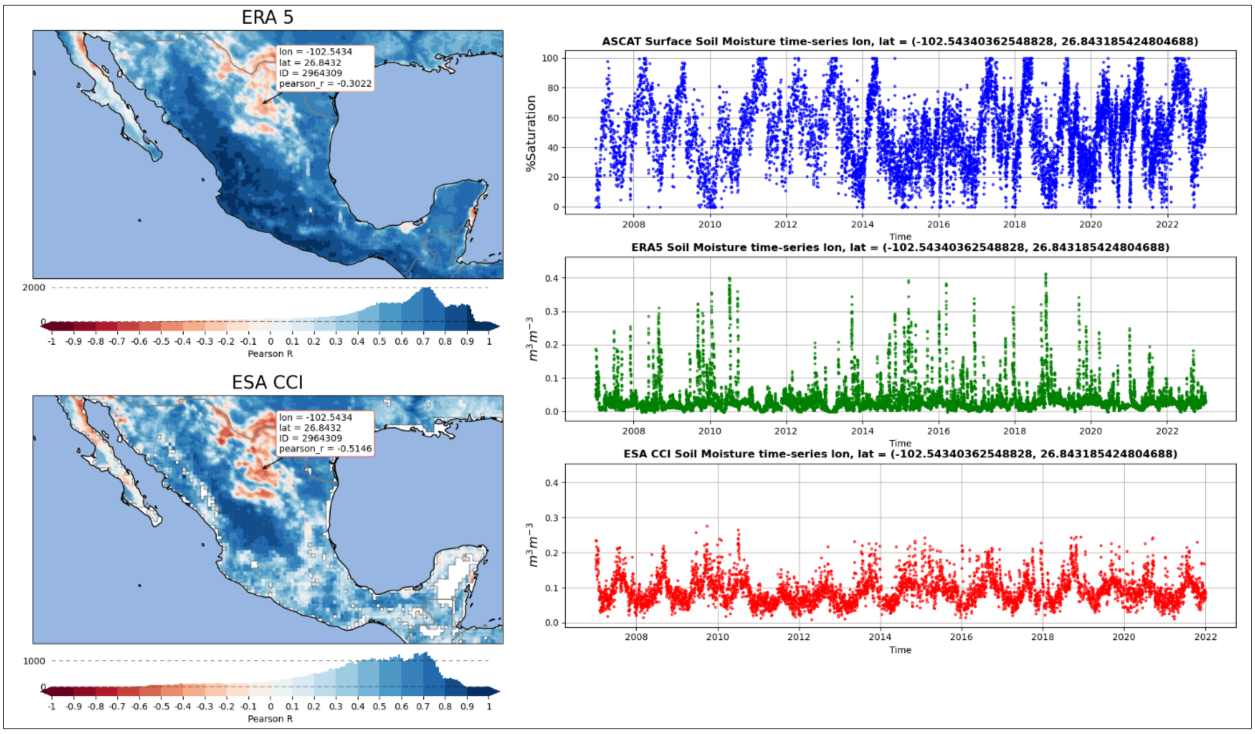

Figure 7. Pearson correlations and time series in arid region in bare land.

The correlations obtained in both points are notably low and negative, ranging from -0.1 to -0.5. Additionally, the time series reveals consistently high soil moisture values, with %Saturation frequently exceeding 40% as measured by ASCAT SSM. The issue of subsurface scattering in these soil types, particularly under arid climatic conditions, has been previously documented in [Wagner et al., 2022].

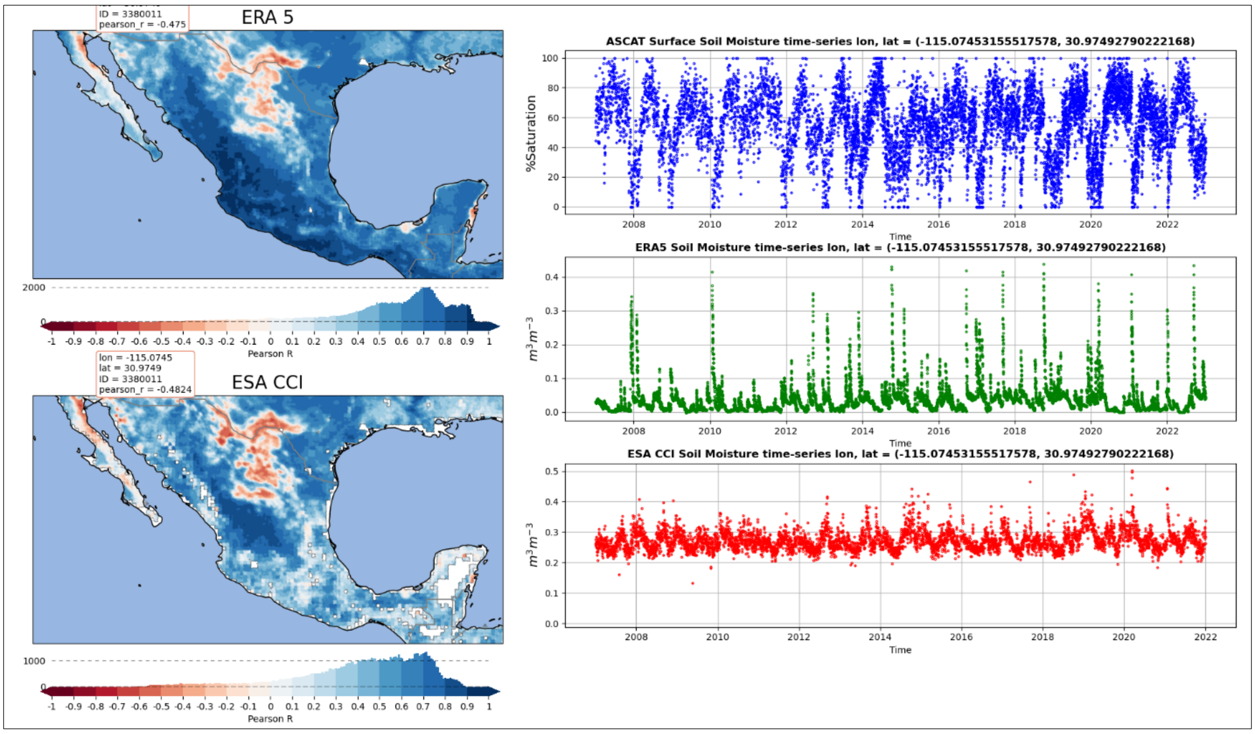

Figure 8. Pearson correlations and times series over bare land arid region in northwest Mexico

As previously mentioned, irrigated areas in arid climates demonstrated low positive correlations. This behavior is evident in Figure 9 and Figure 10, where correlations range between 0.3 and 0.5. The time series in these examples show soil moisture values between 20% and 40% saturation by ASCAT SSM.

Moreover, ERA5 and ESA CCI exhibit soil moisture values ranging from 0.05 to 0.4 m³/m³. This performance appears to be tentatively linked to irrigation, as all three products—ERA5, ESA CCI, and ASCAT SSM—display similar patterns in the time series. This suggests that irrigation may significantly influence the soil moisture values recorded by ASCAT SSM in arid and semiarid regions.

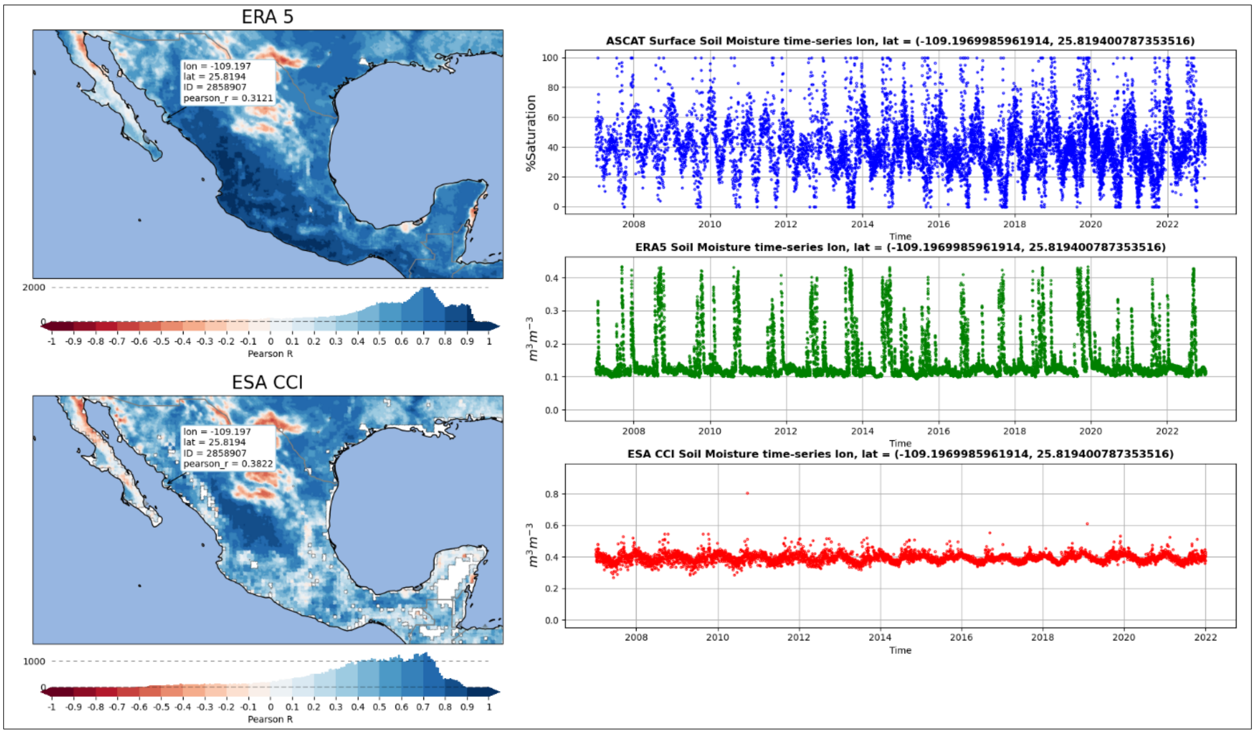

Figure 9 Pearson correlations and times series over irrigated agriculture region in arid climate

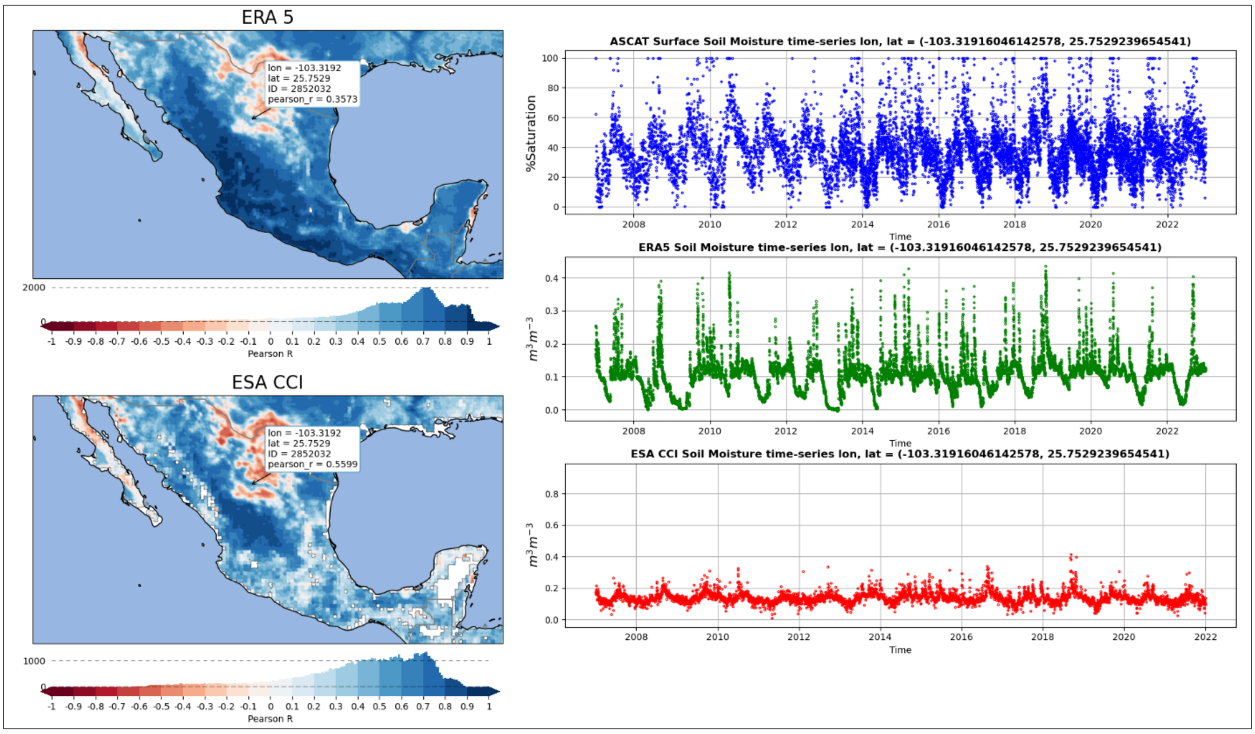

Figure 10 Pearson correlations and times series over arid climate region with irrigation agriculture in north Mexico

Following this analysis of semiarid regions, Northeast Mexico was also examined. Figure 11 shows that correlations in the region generally exceed 0.6, regardless of agricultural activity. This indicates that the Northeast Mexico region is better correlated compared to the semiarid areas in the northwest.

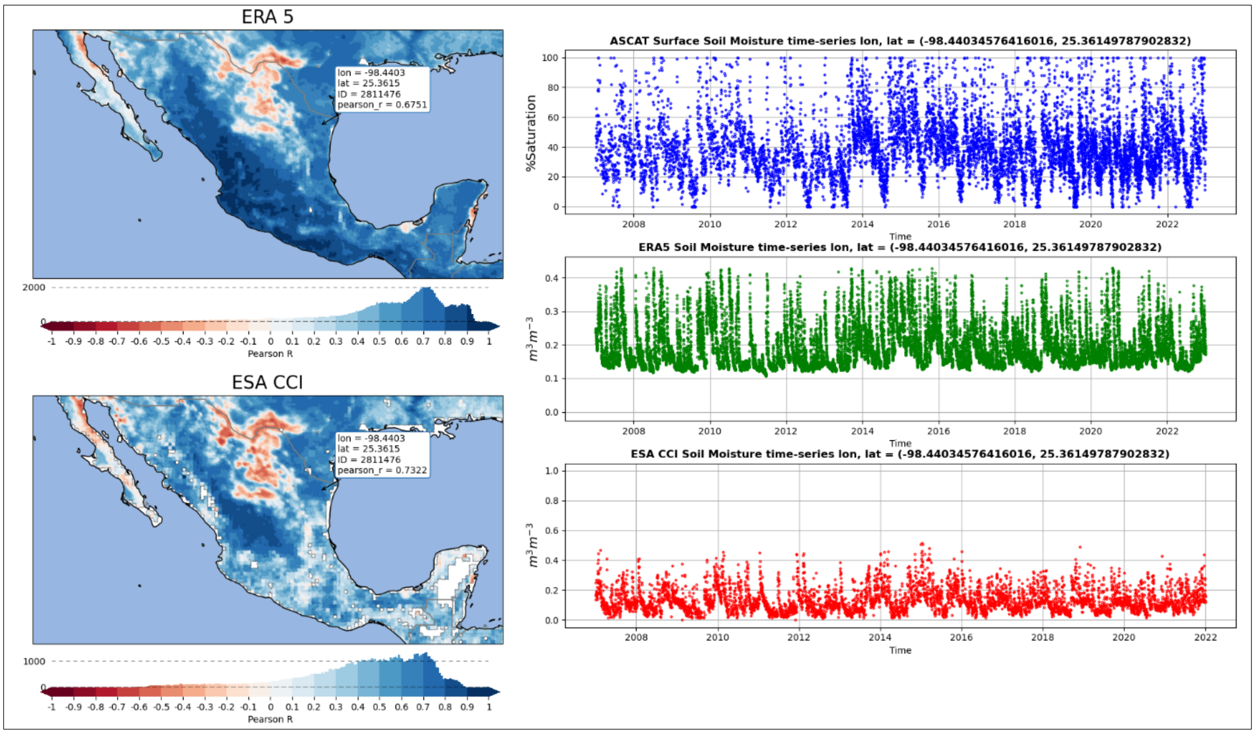

Figure 11 Pearson correlations and times series over semiarid climate region with irrigation agriculture in northeast Mexico

In contrast, central and southern Mexico exhibited strong correlations (0.7 to 0.9) in regions characterized by tropical savanna (Aw) and temperate climates with dry winters (Cwa and Cwb).

The central region, predominantly comprising croplands reliant on rainfall, demonstrated consistent performance. However, as illustrated in Figure 12, certain sectors displayed lower correlations with ESA CCI, primarily due to data gaps within the time series.

Furthermore ERA5, showed high correlations within both bare lands (Figure 12) and croplands areas (Figure 13). Dense forest regions and high-altitude areas also demonstrated robust correlations, with soil moisture values in the time series showing consistent alignment across the various products. Additionally, the time series effectively captured the seasonal variability, representing both dry and wet periods, and showed promise in accurately identifying drought conditions.

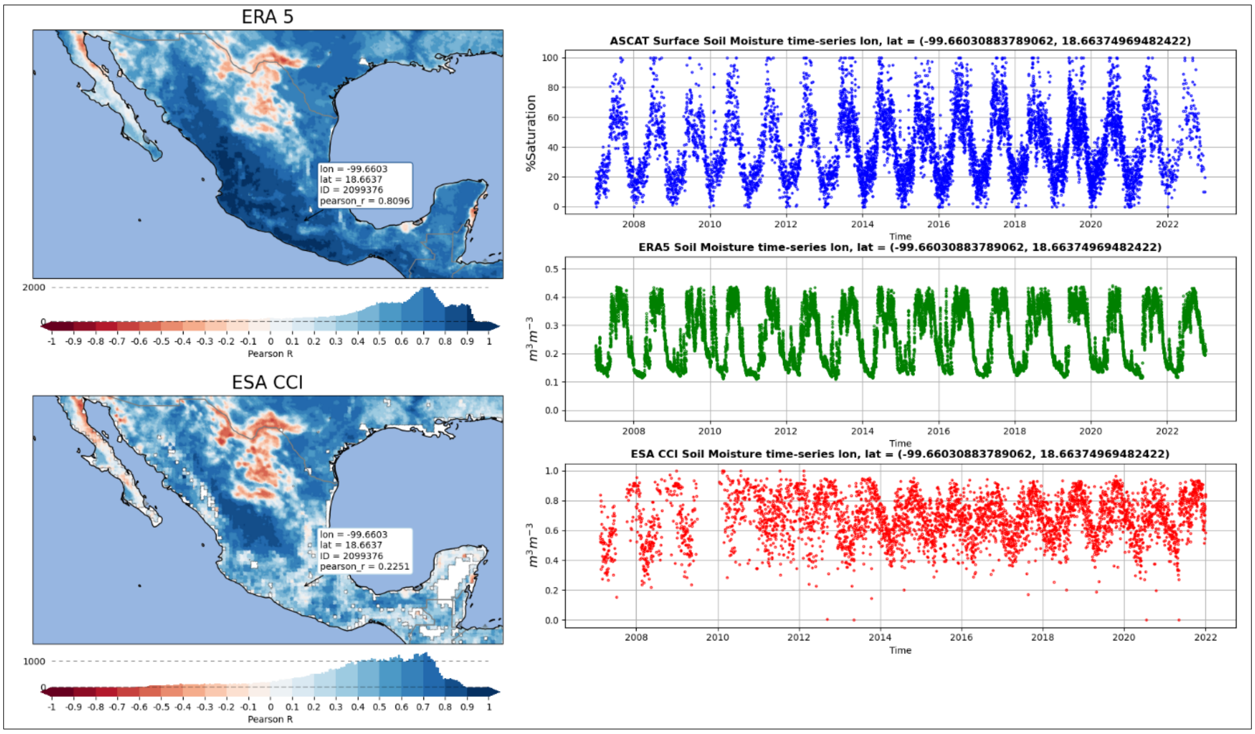

Figure 12 Pearson correlations and times series over central Mexico

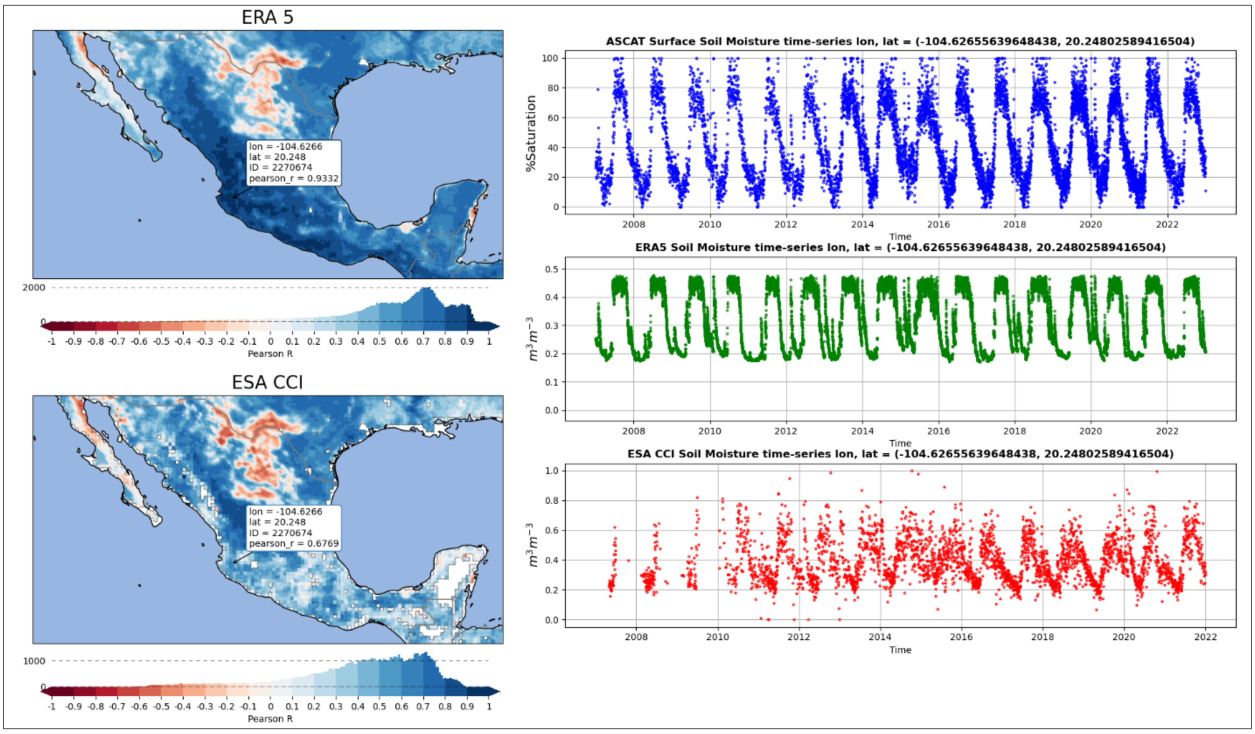

Figure 13 Pearson correlation and time series over agriculture zone in central Mexico

4 Drought indicator assessment

4.1 Introduction

The anomaly approach is ideal for utilizing HSAF SSM data to derive drought indicators. The extended data record of 17 years makes it possible to calculate reliable soil moisture climatology (long-term mean and standard deviations). This, in turn, allows us to determine deviations in soil moisture from normal conditions, representing anomalies in the soil moisture. When anomalies are close to 0, it indicates normal conditions, while negative anomalies indicate drier-than-usual conditions. Positive anomalies, on the other hand, show a surplus of soil moisture in the events of strong precipitation [Vreugdenhil, M., et.al.,2022].

4.2 Comparison of Anomalies

A comparison of Monthly Precipitation Anomalies (MPA), produced by CONAGUA and SMN using rain gauge data, is conducted alongside Soil Moisture Anomalies (SMA) derived from ASCAT surface soil moisture (SSM). This analysis aims to evaluate the consistency between precipitation deficits and soil moisture patterns during the drought years of 2015, 2018, and 2021.

In most months, soil moisture and precipitation anomalies exhibited similar patterns, as shown in Figure 14, Figure 15, and Figure 16. Notably, discrepancies were found only in March 2015 and July 2021. However, exceptions were observed in arid and semi-arid regions, likely due to subsurface scattering issues.

March 2015 exhibited a positive precipitation anomaly across the country (+20 mm); however, Soil Moisture Anomalies (SMA) displayed low values in central and southern Mexico (Figure 14). During the same year, September, February, and August showed the best agreement between SMA and the Monthly Precipitation Anomaly (MPA). Conversely, April and June 2015 demonstrated lower correspondence, with discrepancies primarily occurring in arid and semi-arid regions.

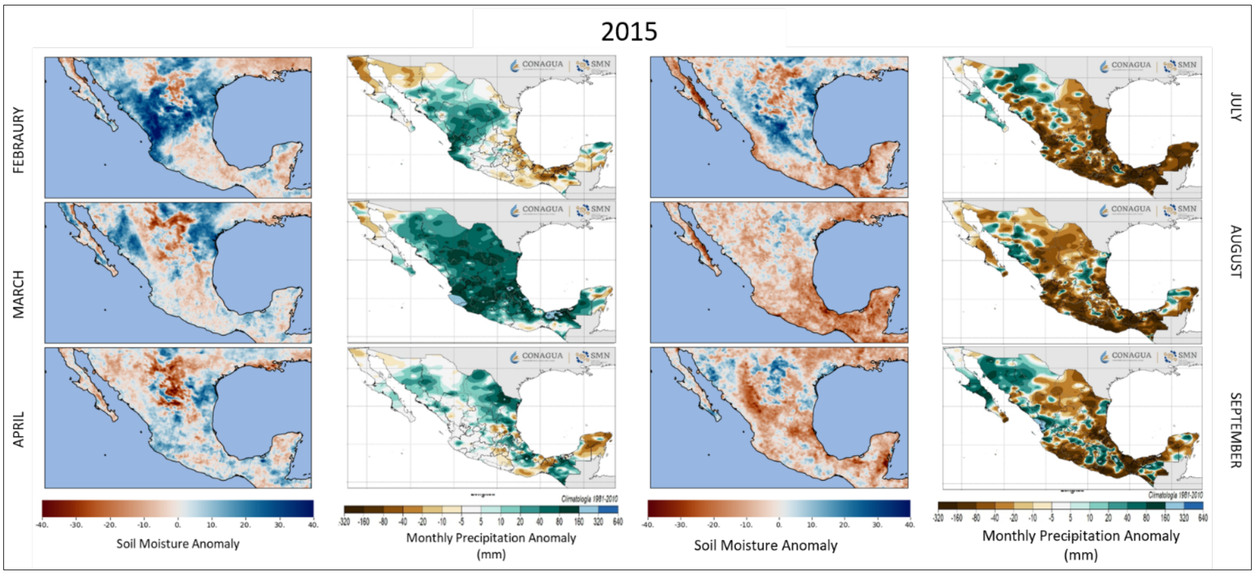

Figure 14 Soil Moisture and Monthly Precipitation Anomalies for dry and wet months, year 2015

Figure 15 illustrates the anomalies for the year 2018, which generally displayed a high degree of similarity, except in April and August. In these months, the SMA did not appear to reflect the presence of precipitation near coastal regions. February and September showed the closest similarity, even in arid and semi-arid areas.

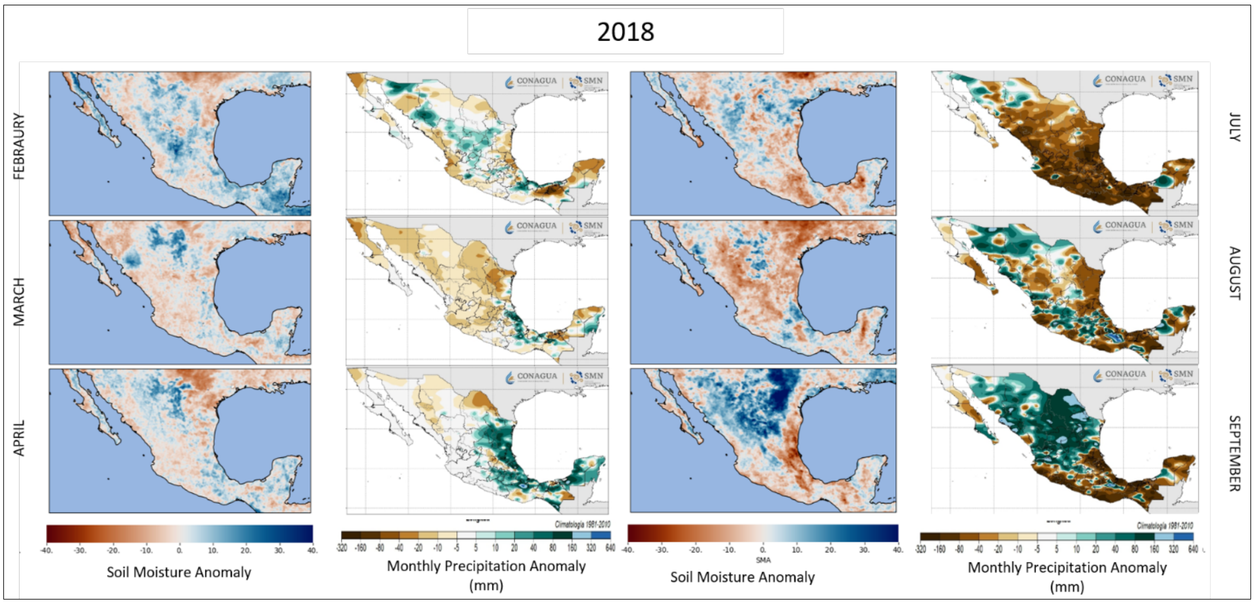

Figure 15 Dry and wet months of 2018 showing Soil Moisture and Monthly Precipitation Anomalies

In 2021, the first five months faced drought conditions, as reported by the Mexico Drought Monitor (MSM). Figure 16, illustrates the dry and wet months of the year. Notably, July exhibits the greatest pattern discrepancies, likely due to the onset of the initial rains following the drought period. Additionally, persistent issues are evident in the arid and semi-arid regions.

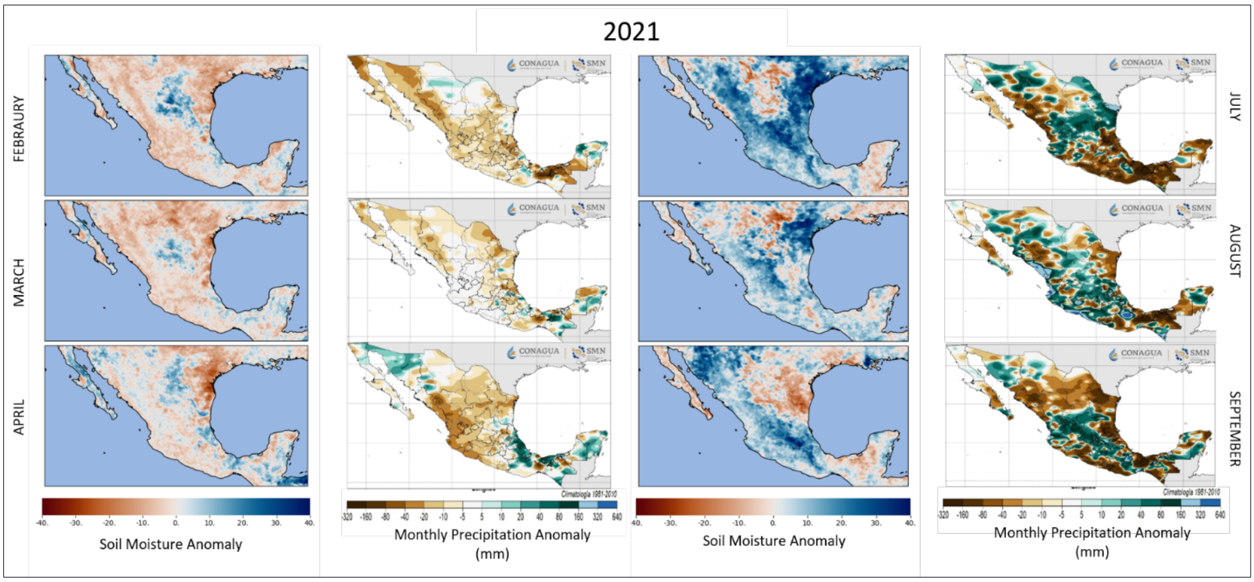

Figure 16 Soil Moisture Anomalies and Monthly Precipitation Anomaly for dry and wet month in year 2021

4.3 Drought Indicators

Droughts are a complex phenomenon, due to their slow onset and slow recovery, the several different drought categories, and their different causes and complex impacts, make droughts events difficult to define quantitatively, giving rise to a multitude of indices.

Drought indices are essential tools for identifying and quantifying drought events. They are typically categorized into standardized indices and threshold-based indices. Among the most used indices are those based on meteorological and soil moisture droughts [Van Loon, A.F., 2015]. The selection and application of a specific index are critical, as these choices can significantly influence the interpretation of drought conditions and may lead to varying conclusions.

The most common standardized drought indices based on meteorological drought monitoring are the Standardized Precipitation Index (SPI) and the Standardized Precipitation and Evapotranspiration Index (SPEI). Both methods use precipitation as their main statistical indicator, based on comparing the total amount of precipitation (mm) during a specific period (months), with a long-term precipitation distribution [Sepulcre-Canto, G..et al. 2012].

On the other hand, the standardized indices for soil moisture drought, use the soil moisture anomalies to standardize them either by calculating the percentage using the long-term means (**SMAPI**) or by calculating **Z-scores** using the long-term standard deviations and then thresholding them to categorize the severity of droughts.

To evaluate ASCAT SM as a drought detection tool in Mexico, four drought indicators were selected: two precipitation-based and two soil moisture-based indicators. Table 1 provides a summary of the methods and classification used for each drought indicator.

Table 1. Drought Indicators

Indicator	Equation	Common thresholds	
Standardized Precipitation Index (SPI)	$SPI = \frac{P - p^*}{\sigma p}$	Normal	0.99 to -0.99
		Moderate	-1.0 to -1.49
		Severe	-1.5 to -1.99
		Extreme	≤ -2.0
Standardized Precipitation and Evapotranspiration Index (SPEI)	$D_i = P_i - PET_i$	Normal	0.99 to -0.99
		Moderate	-1.0 to -1.49
		Severe	-1.5 to -1.99
		Extreme	≤ -2.0
Z-scores	$Z_{k,i} = \frac{SM_{k,i} - \overline{SM_i}}{\overline{\sigma_i}}$	Mild	More than -1
		Moderate	-2 to -1
		Severe	Lower than -2
Soil Moisture Anomaly Percentage		No drought	-5% or more
		Mild	-15% to -5%
		Moderate	-30% to -15%

Index (SMAPI)	$SMAPI_{k,i} = \frac{SM_{k,i} - \overline{SM_i}}{\overline{SM_i}} \cdot 100\%$	Severe	-50% to -30%
		Extreme	More than -50%

Where P represents precipitation, p mean precipitation, and σp standard deviation of precipitation*
Where $SM_{k,i}$ represents monthly soil moisture values and $\overline{SM_i}$ and $\overline{\sigma_i}$ represents long-term monthly means and standard deviations respectively.
For SPEI see [Vicente-Serrano et al., 2010]

4.4 Assessment

The assessment of the quality and effectiveness of drought indicators derived from HSAF SSM data involved a comparative analysis with the Standardized Precipitation and Evapotranspiration Index (SPEI), and the Standardized Precipitation Index (SPI) generated by the Mexico Drought Monitor (MSM). This comparison analysis aimed to evaluate the ability of HSAF SSM-derived indicators to reflect drought severity and duration in a manner consistent with established meteorological indices. Below is an overview of the data products used for the drought indicator assessment.

4.4.1 Overview of products

4.4.1.1 Standardized Precipitation and Evapotranspiration Index (SPEI) [Peng et al., 2023]

SPEI is a multi-scalar drought indicator derived using precipitation and temperature data [Vicente-Serrano et al., 2010] calculated over different accumulation timescales: 1, 3, 6, 12, 18, and 24. The UK Centre for Environmental Data Analysis (CEDA) provides high-resolution SPEI datasets for Africa, which are based on CHIRPS precipitation data and potential evaporation estimates from the Global Land Evaporation Amsterdam Model (GLEAM). These datasets have a spatial resolution of 5km and monthly temporal resolution.

4.4.1.2 Standardized Precipitation Index (SPI): Drought Severity Classification

The Mexico Drought Monitor (MSM, by its Spanish initials) is a monthly report that assesses drought severity across the country using the Standardized Precipitation Index (SPI) [CONAGUA & SMN, 2024]. This report provides a comprehensive overview of drought conditions, supplemented with tables and graphical representations illustrating the percentage of affected areas at the municipal, state, and national levels. It is produced by the National Meteorological Service (SMN) in collaboration with the National Water Commission (CONAGUA), utilizing data from the National Rain Gauge Network, the National Automatic Meteorological Stations Network, and radar observations.

4.4.2 Comparative Analysis

Between 2020 and 2021, Mexico experienced the second most severe drought in recent years. This event spanned from July to December 2020 and continued from January to May 2021. During this period, the country recorded an average precipitation deficit of 2.7%, marking the third (2020) and fourth (2021) consecutive years of below-average precipitation. According to the

Mexico Drought Monitor (MSM), at least 75% of the national territory experienced some grade of drought severity during this time.

Figure 17 illustrates the onset of the drought, as captured by the SMAPI, Z-Scores, SPEI, and SPI indices. During the first three months, both precipitation-based indices showed agreement in several regions. Notably, September exhibited the highest degree of dissimilarity, particularly in northern Mexico. However, Z-Scores demonstrated a stronger resemblance to the SPI compared to the SMAPI.

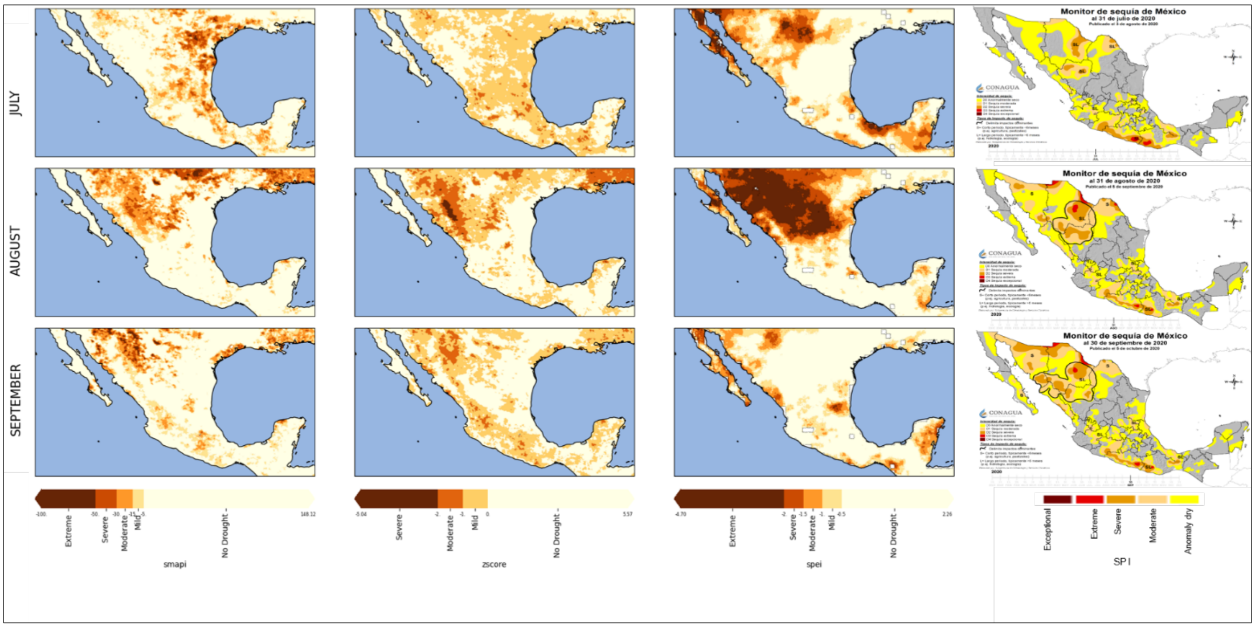

Figure 17.Drought anomalies from July to September 2020

Figure 18 presents the second trimester of the drought, where the alignment of drought-affected areas becomes more evident, particularly in October and November. However, arid and semi-arid regions appear to indicate 'no drought' conditions, likely due to subsurface scattering issues in the ASCAT SSM data.

December appears to exhibit the greatest divergence among the drought indices. The SPEI indicates 'no drought' in most of northern Mexico, similar to certain areas in central and southern Mexico. This contrasts with the MSM's characterization using the SPI, where these regions were identified as experiencing 'severe drought'.

SMAPI and Z-Scores generally exhibited similar patterns to SPI across most of the country, excluding the arid and semi-arid regions. However, discrepancies between the indices persist in western Mexico.

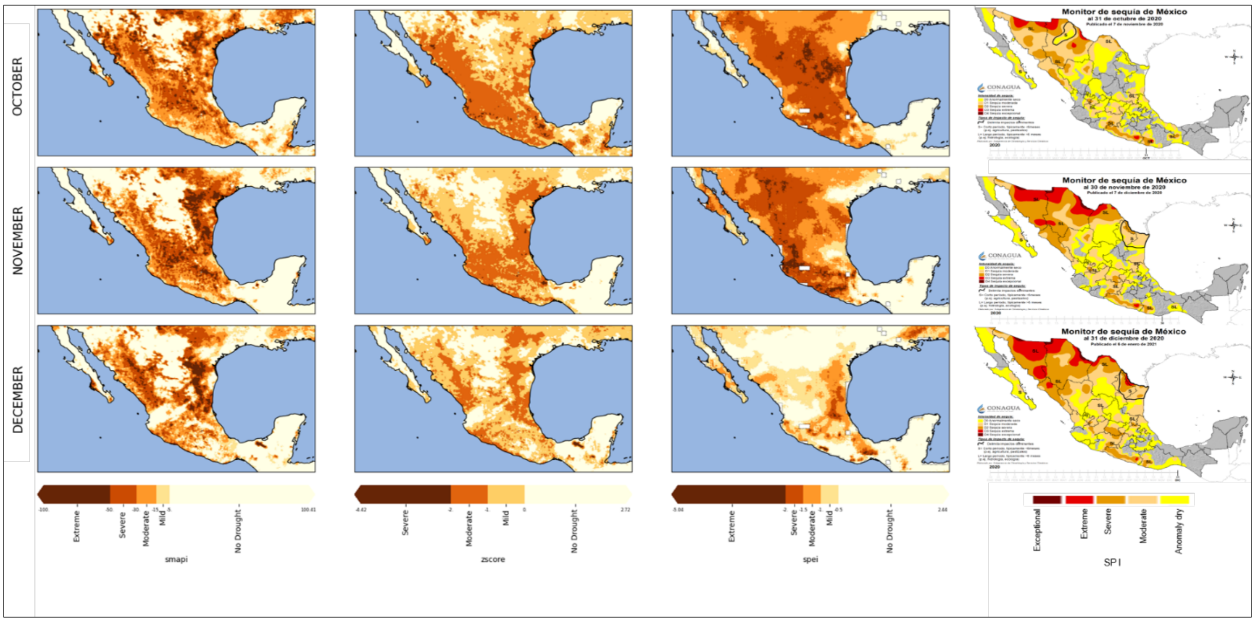

Figure 18. Drought anomalies for the second trimester of drought, from october to december 2020

The third trimester of the drought, as illustrated in Figure 19, revealed moderate to severe SPI indices in the central and northwest regions. Discrepancies between SPEI and SPI were evident in these areas, particularly during January and February. Additionally, SMAPI and Z-Scores are generally aligned with SPI. However, issues in arid regions, notably in the northern central states of Chihuahua and Coahuila, persisted as expected.

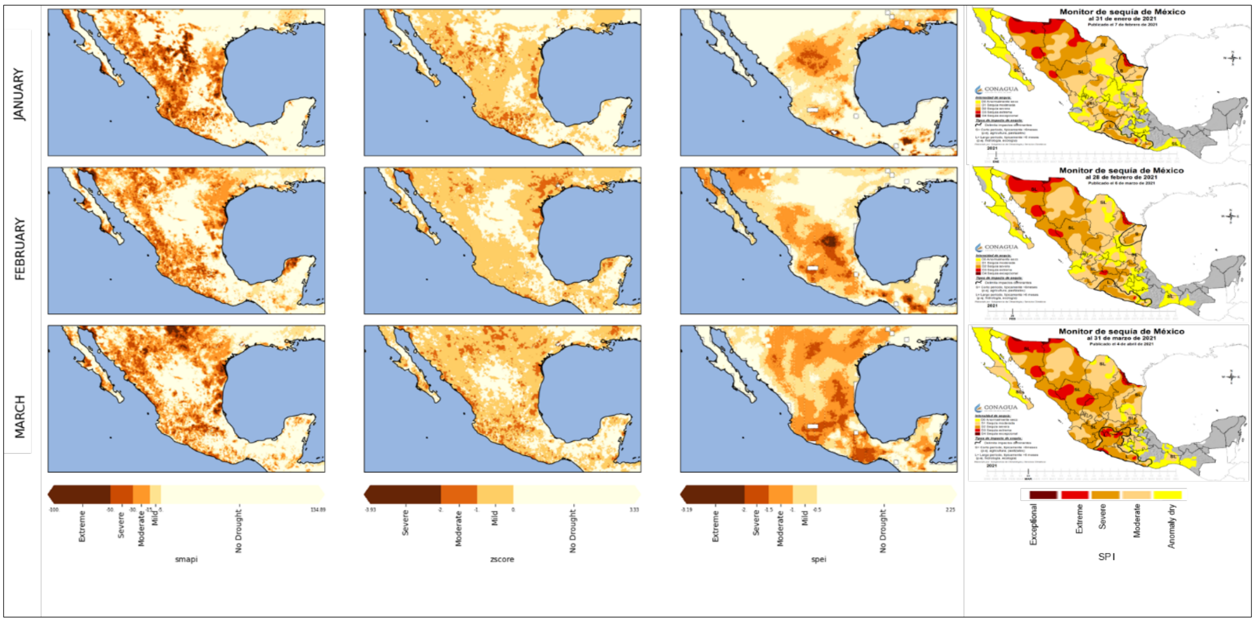

Figure 19. 2021 drought anomalies from January to March

According to the MSM, the drought was reported to have ended in June 2021. However, as shown in Figure 20, northwest Mexico continued to experience 'extreme drought conditions' during June. In contrast, the SPEI indicated 'no drought' conditions, as reported by CONAGUA and SMN. Additionally, SMAPI and Z-Scores indicated mild to moderate drought conditions in areas like those identified by SPI. Conversely, April displayed greater discrepancies among the indices compared to the other two months, with variations not limited to arid and semi-arid regions.

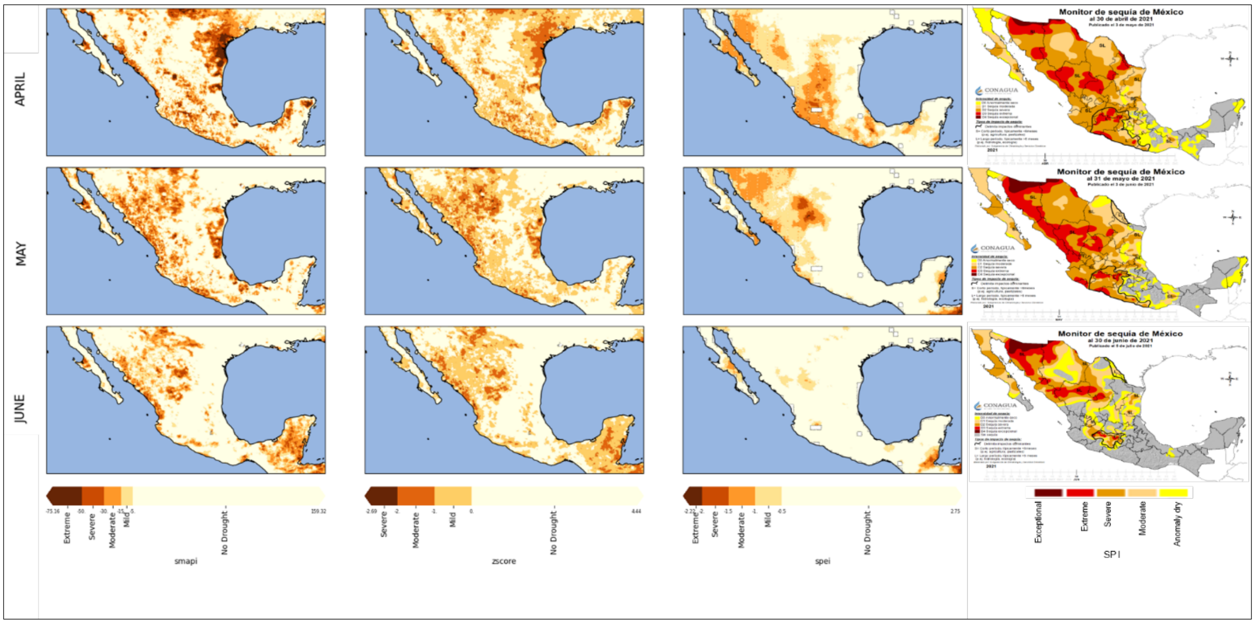

Figure 20. 2021 drought anomalies from April to June

5 Conclusion

This report evaluated the potential of the ASCAT SSM 6.25 km product for agricultural drought monitoring across Mexico. Correlation analyses with other soil moisture datasets confirmed the product's quality while highlighting the impact of subsurface scattering, particularly in the arid regions of Northern Mexico.

Using the ASCAT SSM 6.25 km product, two anomaly-based drought indicators were generated and evaluated for their alignment with precipitation anomalies during historically significant drought events. Additionally, a comparative analysis with the Standardized Precipitation and Evapotranspiration Index (SPEI) and Standardized Precipitation Index (SPI) showed a generally strong correspondence in spatial drought patterns.

Furthermore, SMAPI and SMA Z-score drought indicators effectively captured precipitation deficits and drought conditions, closely mirroring the patterns observed in the MSM SPI. While challenges remain in arid and semi-arid regions, the indicators showed a strong potential for use in central and northeastern Mexico.

6 References

A. Monsiváis-Huertero et al., "Assessment of NASA SMAP Soil Moisture Products for Agricultural Regions in Central Mexico: An Analysis Based on the THEXMEX Dataset," in IEEE Journal of Selected Topics in Applied Earth Observations and Remote Sensing, vol. 15, pp. 3421-3443, 2022, doi: 10.1109/JSTARS.2022.3165078.

CONAGUA & SMN, (2024). Monitor de Sequia en Mexico (MSM). Coordinacion General del Servicio Meteorologico Nacional de la Comision Nacional del Agua. https://smn.conagua.gob.mx/es/climatologia/monitor-de-sequia/monitor-de-sequia-en-mexico

Dorigo, W.A., Wagner, W., Albergel, C., Albrecht, F., Balsamo, G., Brocca, L., …& Lecomte, P. (2017). ESA CCI Soil Moisture for improved Earth system understanding: State-of-the art and future directions, Remote Sensing of Environment. https://doi.org/10.1016/j.rse.2017.07.001.

Hersbach, H., Bell, B., Berrisford, P., Biavati, G., Horányi, A., Muñoz Sabater, J., …&Thépaut, J.-N, 2018. ERA5-Land hourly data from 1950 to present, Copernicus Climate Change Service (C3S) Climate Data Store (CDS) [data set]. https://doi.org/10.24381/cds.adbb2d47

Huerta-Bátiz, H. E., Constantino-Recillas, D. E., Monsiváis-Huertero, A., Hernández-Sánchez, J. C., Judge, J., & Aparicio-García, R. S. (2022). Understanding root-zone soil moisture in agricultural regions of Central Mexico using the ensemble Kalman filter, satellite-derived information, and the THEXMEX-18 dataset. International Journal of Digital Earth, 15(1), 52–78. https://doi.org/10.1080/17538947.2021.2012534

Lobato-Sanchez, R. (2015). Estimación de Humedad de Suelo con base en imágenes de satélite. Proyecto TH1508.1 Subcoordinación de Hidrología Superficial. Instituto Mexicano de Tecnología del Agua. http://repositorio.imta.mx/handle/20.500.12013/1785

Lopez-Quiroz, M., Loranca-Dominguez, Y., Zavala-Fajardo, A.G., Gomez-Camacho, J., Farias-Nunez, O.A., Lopez-Trujillo, J.A., Reyna-Lopez, H., & Lunagomez-Cruz, D.P. (2024). Reporte Annual del Clima en Mexico 2023. Coordinacion General del Servicio Meteorologico Nacional de la Comision Nacional del Agua. Ano 13, Numero 13. https://smn.conagua.gob.mx/es/climatologia/diagnostico-climatico/reporte-del-clima-en-mexico

Peng, J., Dadson, S., Hirpa, F., Dyer, E., Lees, T., Miralles, D. G., Vicente-Serrano, S. M., & Funk, C, (2019). High resolution Standardized Precipitation Evapotranspiration Index (SPEI) dataset for Africa. Centre for Environmental Data Analysis, 05 August 2019. doi:10.5285/bbdfd09a04304158b366777eba0d2aeb. https://dx.doi.org/10.5285/bbdfd09a04304158b366777eba0d2aeb

Sepulcre-Canto, G., Horion, S., Singleton, A., Carrao, H., and Vogt, J.: Development of a Combined Drought Indicator to detect agricultural drought in Europe, Nat. Hazards Earth Syst. Sci., 12, 3519–3531, https://doi.org/10.5194/nhess-12-3519-2012, 2012.

Van Loon, A.F. (2015), Hydrological drought explained. WIREs Water, 2: 359-392. https://doi.org/10.1002/wat2.1085

Vicente-Serrano, S. M., Beguería, S., & López-Moreno, J. I. (2010). A multiscalar drought index sensitive to global warming: the standardized precipitation evapotranspiration index. Journal of climate, 23(7), 1696-1718.

Vreugdenhil, M., Greimeister-Pfeil, I., Preimesberger, W., Camici, S., Dorigo, W., Enenkel, M., ... & Wagner, W. (2022). Microwave remote sensing for agricultural drought monitoring: Recent developments and challenges. *Frontiers in Water*, *4*, 1045451.

Wagner, W., Hahn, S., Kidd, R., Melzer, T., Bartalis, Z., Hasenauer, S., ... & Komma, J. (2013). The ASCAT soil moisture product: A review of its specifications, validation results, and emerging applications. Meteorologische Zeitschrift, 22(1), 5-33.

Wagner, W., Lindorfer, R., Melzer, T., Hahn, S., Bauer-Marschallinger, B., Morrison, K., ... & Vreugdenhil, M. (2022). Widespread occurrence of anomalous C-band backscatter signals in arid environments caused by subsurface scattering. Remote Sensing of Environment, 276, 113025.

W. Wagner et al., "Global Scale Mapping of Subsurface Scattering Signals Impacting ASCAT Soil Moisture Retrievals," in IEEE Transactions on Geoscience and Remote Sensing, vol. 62, pp. 1-20, 2024, Art no. 4509520, doi: 10.1109/TGRS.2024.3429550.